Oxygen adsorption on Cu/ZnO(0001)-Zn

Paola Lazcano,[1,2] Matthias Batzill,[3] Ulrike Diebold,[4] and Patricio Häberle[2]
[1]*Departamento de Física, Pontificia Universidad Católica de Valparaíso, Avenida Brasil, 2950 Valparaíso, Chile*
[2]*Departamento de Física, Universidad Técnica Federico Santa María, Avenida España, 1680 Valparaíso, Chile*
[3]*Department of Physics, PHY 114, University of South Florida, 4202 East Fowler Avenue, Tampa, Florida 33620-5700, USA*
[4]*Department of Physics, Tulane University, New Orleans, Louisiana 70118, USA*
(Received 5 February 2007; revised manuscript received 7 September 2007; published 29 January 2008)

We hereby describe the modifications induced in a Cu thin film induced by different oxidation processes. By using plasma assisted deposition, we have adsorbed oxygen onto the Cu/ZnO(0001)-Zn surface. Cu was deposited on the sputtered-annealed ZnO substrate at room temperature, which was later exposed to oxygen. Using x-ray photoelectron spectroscopy, we verified the effect of the surface treatment on the electronic structure. Our findings are consistent with a partially oxidized Cu layer, with the CuO located at the interface between ZnO and the adsorbed Cu islands. Further Cu deposition induces the formation of Cu_2O as judged by the evolution of the spectra. Annealing the sample up to 750 °C in UHV induces further reduction of the oxide, metallic Cu is recovered on the top layer, with evidence of Cu desorption into the vacuum or incorporation into the substrate.

DOI: 10.1103/PhysRevB.77.035435 PACS number(s): 82.45.Jn, 73.22.−f

INTRODUCTION

The Cu/ZnO system has been extensively studied primarily because of its importance as a heterogeneous catalyst for methanol synthesis[1–8] and the reverse water gas shift reaction[6–9] for hydrogen production. Furthermore, solid state gas sensors utilize the CuO/ZnO interface as the active element in humidity sensors[10–12] and also in the detection of harmful gases.[12–15] In these sensors, the fact that copper oxide is a *p*-type material, while ZnO is mostly a *n*-type one, is important for their functionality. Band bending induced at the *p*-*n* junction reduces the conductivity of ZnO. Upon the reaction of CuO with a test gas, the magnitude of these band bendings is modified on the ZnO substrate. This effect causes a modification of the conductivity, which can then be easily monitored and used as the "gas response" signal.

For an improved understanding of the functionality of the Cu/ZnO system in device applications as the one described above, a better characterization of the Cu/ZnO interface is certainly desirable. In particular, the dependence of the interface electronic structure on the oxidation state of copper is a relevant piece of information. To this end, we performed x-ray photoelectron spectroscopy (XPS) studies of Cu deposits on a single crystal ZnO(0001) substrate under ultrahigh vacuum conditions. Different oxidation states of copper were prepared by using an oxygen-plasma source. The *in situ* sample preparation and characterization procedure enables a detailed look on how the interface properties are altered by the interaction with oxygen.

Previous surface science studies of Cu deposition on single crystal ZnO substrates are slightly controversial. One study showed that the growth of Cu proceeds via a two-dimensional mechanism up to a critical coverage of 33% of a monolayer, and then it converts into a three-dimensional (3D) cluster growth.[16,17] Scanning tunneling microscopy (STM) studies, performed by members of our group, demonstrated instead that the growth proceeds by the formation of 3D structures, already at very low Cu coverage.[18] It has been suggested that this discrepancy arises from the Cu growth being very sensitive to the substrate preparation and traces of contaminants at the surface. These differences already hint that small amounts of adsorbed oxygen may play a role in the morphology of Cu clusters. Raimondi *et al.* have investigated the morphological changes induced by different (oxidizing) reaction conditions on a model catalyst consisting of Cu particles supported on a polycrystalline ZnO film, grown on a Si substrate.[19] XPS and atomic force microscopy studies demonstrated that, in the absence of water, the formation of Cu^+ (Cu_2O) proceeds through the formation of islands with a large lateral extent, covering most of the ZnO substrate. On the other hand, in the presence of water, the formation of Cu^{2+} caused an even larger dispersion of the Cu-island size, which resulted in a higher fraction of the ZnO surface being covered by Cu.

Recently, experimental efforts for understanding the Cu/ZnO interface have found support from density functional theory calculations. Meyer and Marx studied Cu adsorption on the two polar surfaces.[20] They found that Cu atoms adsorb on top sites over oxygen on the O-terminated surface, while they preferentially occupy hollow sites for the Zn-terminated surface. This last result can be rationalized by Cu adopting the role of the next Zn layer on the O-terminated face, while on the Zn-terminated surface, the Zn atoms can be viewed as the first layer of a metal film and Cu acts as the continuation of the film, forming Cu–Zn bonds. Bromley *et al.* have also studied Cu on the ZnO(0001)-Zn surface, concentrating primarily on the effect of the different oxidation states of adsorbed Cu.[21] Their results show that Cu is strongly bound to the surface at Zn-vacancy sites, forming anchors for subsequent Cu-cluster growth. A high abundance of Zn vacancies is expected for the Zn-terminated surface as part of the stabilization mechanism of the polar surface.[22,23] For higher oxidation states, the binding energy (BE) increases and Cu^{2+} is the species more strongly bound to the Zn-vacancy sites. The lowest unoccupied molecular orbital of these Cu^{2+} ions is, however, below

the valence band maximum of ZnO, suggesting an electronic transfer to the Cu site, possibly reducing it to Cu^+.

EXPERIMENT

The experiments were carried out under ultrahigh vacuum conditions, in a system consisting of (i) a preparation chamber, with a base pressure of 6×10^{-10} mbar, where the samples were cleaned, metallized, and subsequently oxidized, and (ii) an analysis chamber containing the XPS, operated at a base pressure of 4×10^{-10} mbar.

The ZnO single crystals, mechanically polished and oriented to within 0.5° of the *c* axis of ZnO, were obtained from MTI Corporation. The sample's polarity was confirmed *ex situ* by their chemical etching behavior (the O-terminated face of ZnO etches more rapidly in a HCl solution than the Zn face). They were cleaned, *in situ*, by cycles of Ar^+ ion bombardment (1 keV) at room temperature and annealing up to 700 °C, until no contamination could be detected by XPS.

Cu (99.999 purity) was vapor deposited onto the clean sample at room temperature using a Knudsen effusion source (K cell). The substrates were placed approximately 10 cm away from the source during Cu evaporation. The temperature of the cell was held constant at 1100 °C during Cu deposition.

The deposition rate was calibrated by a quartz crystal microbalance before growth. Deposition rates of 0.008, 0.043, and 0.016 Å s^{-1} were used in all the experiments for Cu films 0.3, 1, and 5 ML (monolayer) thick, respectively. Sample oxidation was carried out at room temperature using an oxygen mini plasma source (OSMiPlas Oxford Scientific), which was operated with an oxygen pressure of 5.5×10^{-6} mbar and a current of 12 mA. The exposure time was 15 min.

The coverage of the deposited metal is given in monolayer equivalent. 1 ML$=1.7\times10^{15}$ atoms corresponds to the number of Cu atoms per unit area in a Cu(111) plane. The typical deposition rate used in this work was 0.42 ML/min. The pressure during Cu deposition remained below 6×10^{-9} mbar, which is only slightly higher than the normal operating pressure.

All the XPS spectra reported here were obtained using an x-ray source (VG XR3E2) with nonchromatized Al $K\alpha$ x-ray radiation (1486.6 eV). A Specs PHOIBOS 100 hemispherical electrostatic energy analyzer with a channeltron energy detector was used, in the medium magnification mode, which gives an acceptance angle of up to ±7° for a 2 mm spot size. This analyzer has a typical energy resolution of 15 meV. The energy scale was calibrated using the $3d_{5/2}$ photoemission peak from a Ag foil. The detection was performed along the surface normal, except when a different angle is explicitly specified. The angle between the x-ray source and the analyzer is fixed at 55° for all measurements.

RESULTS AND DISCUSSION

Previous studies by STM of Cu growth on ZnO (Refs. 17, 18, 24, and 25) showed the formation of well defined clusters. For moderately high Cu coverages, Cu(111) low-energy

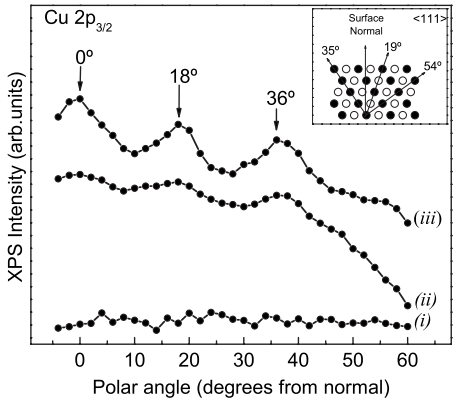

FIG. 1. ARXPS of Cu $2p_{3/2}$ after depositing (i) 0.3 ML, (ii) 1 ML, and (iii) 5 ML at room temperature on the clean ZnO(0001)-Zn surface. Starting at 1 ML coverage, the XPS intensity shows diffraction features consistent with a crystalline ordering of the Cu clusters. The inset shows the angles for the strongest forward focusing peaks expected for a Cu(111) crystal which is oriented azimuthally in the plane along the $\langle\bar{1}100\rangle$ substrate direction.

electron diffraction (LEED) spots were observed, indicating a strict crystallographic relationship of the Cu clusters with respect to the ZnO substrate. In order to probe the crystalline nature of the Cu deposits on our sample, we performed x-ray photoelectron diffraction studies along the $\langle\bar{1}100\rangle$ azimuth of the ZnO substrate. The Cu intensity variations ($2p_{3/2}$) versus the polar angle were monitored after depositing 0.3, 1, and 5 ML at room temperature on the clean ZnO(0001)-Zn terminated surface. The results of these measurements are shown in Fig. 1. For 0.3 ML [trace (i)], the deposited film shows no special features as a function angle, beyond the instrumental resolution. At 1 ML [trace (ii)], two weak peaks appear at 18° and 36°, respectively. Both peaks show a higher intensity for 5 ML [trace (iii)]. No variations in the intensity as a function of angle are expected for emission from an atomically flat surface below 1 ML coverage if the Cu atoms are distributed in a uniform film or if they form a locally disordered thicker Cu film. The fact that we see two weak peaks at 1 ML coverages is an indication of cluster growth. If the clusters are formed by Cu(111) nanoscale crystals, with the $\langle111\rangle$ direction along the surface normal, and azimuthally oriented in the plane, with one of the high symmetry directions along the $\langle\bar{1}100\rangle$ substrate directions, the strongest forward focusing peaks are expected at 19° and −35° (inset in Fig. 1). We see both peaks for positive values of the detection angle, indicating that both possible orientations of the copper clusters are formed during growth. For both of these cluster orientations, the $\langle111\rangle$ direction is parallel to the substrate normal, but the $\langle11\bar{2}\rangle$ azimuth is either parallel or antiparallel to the ZnO $\langle1\bar{1}00\rangle$ direction.

These results are consistent with previous measurements for thicker layers (>5 ML), in which Cu(111) LEED spots have been observed in addition to the ZnO substrate maxima.[25] Yoshihara *et al.*[16] have studied the variation of the Cu $2p_{3/2}$ peak intensity as a function of polar angle along the same azimuth at low coverages (0.41 and 0.98 ML). Their

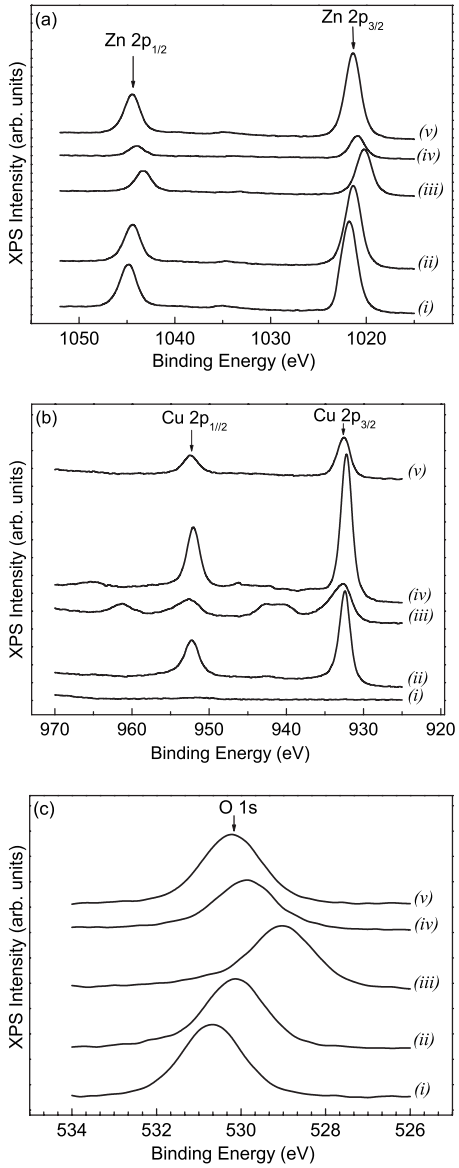

FIG. 2. XPS spectra of (a) Zn $2p$, (b) Cu $2p$, and (c) O $1s$ for (i) ZnO(0001)-Zn clean surface, (ii) after depositing 3 ML Cu, at room temperature, (iii) the same sample after oxidation in oxygen plasma at 10^{-6} mbar, (iv) after an additional deposition of 3 ML Cu on the previously oxidized sample, and (v) the sample annealed to 750 °C. Clear differences are evident between CuO and Cu_2O features in the spectra.

results indicate no special angular variation for both coverages. Only after a slight annealing of the higher coverage film, to 370 K, a weak diffraction feature is detected at about 35°, consistent with (111) growth.

Figure 2 shows the XPS spectra of Zn $2p$ [Fig. 2(a)], Cu $2p$ [Fig. 2(b)], and O $1s$ [Fig. 2(c)] for different preparation conditions; traces labeled by (i) in all graphs correspond to ZnO(0001)-Zn clean surface, (ii) the surface after depositing, at room temperature, 3 ML of Cu, (iii) the same sample after oxidation in an oxygen plasma at 10^{-6} mbar, (iv) after an additional deposition of 3 ML of Cu on the previously oxidized sample, and (v) the sample annealed to 750 °C.

The Zn $2p_{1/2}$ and $2p_{3/2}$ features from the clean ZnO(0001)-Zn surface [trace (i), Fig. 2(a)], obtained after several cleaning cycles, are the two narrow peaks with BEs of 1044.8 and 1021.8 eV and full width at half maximum (FWHM) of 1.88 and 1.93 eV, respectively. From Fig. 2(c), trace (i), we can obtain similar information from the O $1s$ peak. The corresponding BE is 530.6 eV and the FWHM is 1.67 eV.

These Zn $2p$ peaks, with very narrow and symmetrical shapes, show an attenuation of their intensities after every treatment, induced both by the Cu overlayer and the oxygen exposure [traces (ii), (iii), and (iv)]. The peaks are also shifted to lower BEs, for the treatments in (ii), (iii), and (iv), with respect to their clean surface values (see Table I). After annealing the oxidized sample to 750 °C, the intensities of the peaks, as well as the BE and FWHM, are similar to those in (ii), i.e., after the deposition of 3 ML of Cu.

After depositing 3 ML Cu, at room temperature, the trace labeled as (ii), in Fig. 2(b), displays two narrow peaks with FWHM of 1.6 and 1.9 eV, respectively, and BEs of 932.4 and 952.2 eV. These two transitions are the characteristic $2p_{1/2}$ and $2p_{3/2}$ states of metallic Cu.[26] The substrate-related O $1s$ peak [Fig. 2(c), trace (ii)] is fairly narrow (1.63 eV) and symmetrical. It also shifts with respect to the oxygen peak in the clean ZnO surface to a lower BE (530.2 eV). The fact that this system has two components (ZnO and Cu), and both the O and Zn features shift their energies by the same amount (−0.4 eV) upon Cu deposition, without changing significantly the peak shapes, points toward a band bending mechanism instead of a chemical shift as the reason for these BE modifications.

Consistent with our results, Yoshiuara *et al.*[16] reported a reduction in the binding energy of the Zn $2p_{3/2}$ of 0.05 eV for 0.3 ML Cu and 0.25 eV for a coverage of 1 ML. For the same coverages, Didziulis *et al.*[27] reported an upward band bending of 0.15 and 0.3 eV, respectively. They did not show results for higher coverages. In Fig. 3, we display the energy shifts in the binding energy due to Cu deposition for coverages as large as 10 ML. The deposition of Cu on ZnO(0001) produces only an upward band bending. The fact that the bands need to be bent upward to align the vacuum levels agrees with the fact that the work function of ZnO is smaller than that of Cu. From various references, the different values reported for the work function are 3.5–3.9 eV,[16] 3.9 eV (Ref. 27) for ZnO(0001), and 4.6–4.9 eV for Cu,[27] in agreement with the sign and magnitude of the band bending we can infer from our own data, for the Cu/ZnO system.

In the following paragraphs, we examine the modifications of the electronic structure of the Cu clusters induced by the different sample preparation procedures, as shown by the spectra in Fig. 2(b). The effect of oxygen exposure [trace (iii)] induces both a shift and a broadening when compared to the previous spectrum [trace (ii)]. The Cu $2p$ peaks present a visible broadening on the higher BE side. Since the core-level BE of an atom is closely related to its chemical environment, this additional intensity could then be interpreted as a chemical shift associated with some of the Cu atoms in the overlayer being in a different chemical state. It is also fair to point out that inhomogeneous surface charging in the thin layer could also induce a similar broadening, but we are

TABLE I. BE of Zn $2p_{3/2}$ and O 1*s* features for (i) clean surface, (ii) after depositing 3 ML Cu at room temperature, (iii) the same sample after an oxidation treatment in oxygen plasma at 10^{-6} mbar, (iv) after an additional deposition of Cu on the previously oxidized sample, and (v) after the sample was annealed to 750 °C. The labels in parentheses correspond to the treatments described in Figs. 2 and 4.

	Zn $2p_{3/2}$			O 1*s*					
Treatment	BE (eV)	FWHM (eV)	Peak area (cps)	BE (eV)		FWHM (eV)		Peak area (cps)	
(i)	1021.8	1.93	532763	530.6		1.67		92963	
(ii)	1021.4	1.91	509000	530.2		1.63		84449	
(iii)	1020.2	1.87	279284	529.0	529.3	1.55	2.0	49237	31254
(iv)	1020.8	1.78	130962	529.6	530.2	1.30	1.55	23851	36737
(v)	1021.4	1.89	512109	530.2		1.62		86009	

discarding this possibility since no evidence to this effect have been found of such behavior in previous studies.

At this point, we have assumed this peak (Cu $2p_{3/2}$) to be formed by two components which we have fitted to the raw data. One of them at 932.4 eV, corresponds to metallic Cu and the second one, at 933.7 eV, to CuO,[26,28–31] as shown by previous measurements. Table II shows a summary of different parameters obtained for the Cu $2p_{3/2}$ features obtained from the traces in Fig. 2(b). To help in the identification of the different spectral features, we have also presented in Table III a compilation, from different sources in the literature, of the BE of copper and oxygen features as measured by XPS.

In addition to the broadening, a complex satellite peak structure develops a few electron volts above the corresponding core-level positions. The 942 eV satellite feature is linked to the $2p_{3/2}$ transition and has a FWHM of 3 eV ($2p_{1/2}$:961 eV, FWHM 2.5 eV). These additional intensities can be described as shake-ups,[26,32,33] as they occur when the outgoing photoelectron simultaneously interacts with a valence electron and excites it ("shakes it up") to a higher-energy level. The kinetic energy of the core-derived electron is then reduced slightly, giving rise to a satellite structure a few electron volts above the main peak in a BE scale. In this system, these strong shake-up satellite peaks are considered an unequivocal signature for the presence of CuO (Refs. 26 and 28–34) in the sample.

After a new deposition of 3 ML Cu [trace (iv)] on the previously oxidized sample, we detect additional changes in the Cu 2*p* spectra. Both satellite peaks related to CuO (942 and 961 eV) disappear, the 2*p* transitions become narrower and symmetrical again, namely, the high-energy shoulder is strongly attenuated. The new Cu $2p_{3/2}$ and $2p_{1/2}$ BEs are 932.2 and 952.0 eV, respectively. Additionally, two small features appear at about 946.3 and 964.5 eV BE. They have been identified as characteristic satellites of Cu 2*p* in Cu_2O.[28,30,31,33–35]

Annealing the oxidized sample to different temperatures between 400 and 750 °C reduces gradually the intensity of the satellite peaks associated with Cu_2O. Finally, upon annealing to 750 °C, this feature is almost imperceptible [trace (v), Fig. 2(b)) in the data. The shape of the Cu $2p_{3/2}$ feature at 932.2 eV [trace (iv)] remains almost unaltered after annealing, but the whole peak gets shifted to a higher BE: 932.6 eV, when the temperature goes as high as 750 °C.

It is tempting to conclude then that we have recovered metallic Cu on top of the ZnO substrate after the reduction process is completed. It is also evident that Cu desorbs into the vacuum, as reflected by the reduction of the corresponding Cu 2*p* peak area in trace (v) [Fig. 2(b)]. Nevertheless, additional insight is provided by the Cu LMM Auger transitions as displayed in Fig. 4. The trace labels in Fig. 4 are in a one to one correspondence with those shown in Fig. 2. The salient feature in the spectra after depositing Cu on the clean ZnO substrate is the appearance of a peak at a kinetic energy of 918.5 eV [trace (ii)]. Oxygen exposure does not change the BE of this feature [trace (iii)] even though it changes its width. A more detailed analysis shows that this peak has two components, one most likely related to Cu (918.6 eV KE) and a second one derived from CuO (917.8 eV KE). Further Cu deposition induces additional changes in the spectrum [trace (iv)]. The LMM transition now becomes stronger and is also shifted to 916.6 eV KE. As a summary in Table III, we display, from different sources in the literature, the KE of Cu LMM as measured by XPS.

Since the 2*p* BEs of the oxidized Cu^+ and reduced Cu have very similar values, it is hard to distinguish one from the other just by looking at this resonance. However, the substantial difference between traces (ii) and (iv) in Fig. 4,

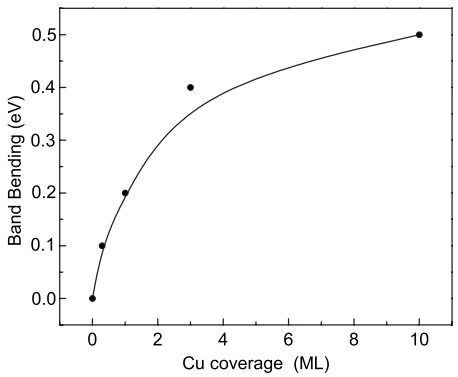

FIG. 3. Cu deposition on ZnO(0001) induces a reduction in the binding energy of the Zn $2p_{3/2}$ peak. Consistently the band bending increases as a function of Cu overlayer thickness.

TABLE II. BE for Cu $2p_{3/2}$ for (i) clean surface, (ii) after depositing 3 ML Cu at room temperature, (iii) the same sample after an oxidation treatment in oxygen plasma at 10^{-6} mbar, (iv) after an additional deposition of Cu on the previously oxidized sample, and (v) after the sample was annealed to 750 °C.

Treatment	BE (eV)		FWHM (eV)		Peak area (cps)	
(ii)	932.4		1.6		236122	
(iii)	932.4	933.7	2.3	2.9	89075	59136
(iv)	932.2		1.6		373511	
(v)	932.6		1.8		114778	

together with the satellite structure in Fig. 2, seems to confirm that Cu deposition, on a partially oxidized CuO layer, induces the formation of Cu_2O. The Auger LMM lines,[30,31] which show shifts under the different treatments, allow an easier differentiation between Cu and Cu_2O, which would not be evident just from detecting the changes in the Cu 2*p* core-level spectra.

In the Auger spectrum of the "reduced" film [Fig. 4, trace (v)], the clear and sharp Cu Auger feature, present in the as-deposited sample, is replaced, in the annealed sample, [ZnO(0001)/Cu/O/Cu-annealed; Fig. 4, trace (v)] by a fairly broad resonance barely distinguishable from the ZnO background. These Auger features, together with the shape, BE, and width of the Cu 2*p* resonance [Fig. 2(b)], show that the annealing procedure reduces the Cu_2O on the surface to metallic Cu with a considerable desorption into the vacuum or possibly cluster coalescence, consistent with an increased contribution of ZnO in the corresponding Auger spectrum. From the data available, it is not possible to differentiate between these alternatives.

The changes in the Cu peaks are also accompanied by modifications in the oxygen spectra, as shown by the corresponding traces in Fig. 2(c). After oxygen exposure, the O 1*s* peak [trace (iii)] becomes broader and asymmetrical, with a shoulder on the high BE side. This broadening is consistent with the presence of more than one type of oxygen in the interfacial region (ZnO and CuO). As a first approximation, we fitted two components to this peak: one related to the substrate and the other one to CuO.

As a reference, to identify the band bending associated with changes in the surface carrier concentrations,[36] we used the Zn 2*p* BE shift and assumed the same value for the O 1*s* feature, as expected for photoelectrons emerging from a common surface. As seen in the data summarized in Table I, the Zn $2p_{3/2}$ BE decreases by 1.6 eV after O_2 exposure. Consistent with this shift, the ZnO component of the O 1*s* peak should be at 529.0 eV. The second component, associated with the broadening, is then determined by the best fit to the data. In this case, the BE related to the presence of CuO on the surface is 529.3 eV. The assignment of the characteristic BEs to different oxidation states of copper is better understood by comparing our data with previous measurements, as those shown in Table III. These values, together with the changes displayed by the Cu 2*p* peaks, are in agreement with the formation of CuO in the adsorbed layer.

After an additional deposition of 3 ML Cu on the previously oxidized sample [Fig. 2(c), trace (iv)], the O 1*s* peak shifts to a slightly higher binding energy and becomes narrower and more symmetrical. To determine the components of this peak, we used the same procedure described in the previous paragraph. From this procedure, the BE of the substrate-related component is at 529.6 eV, and the oxide (Cu_2O) related feature has a BE of 530.2 eV.

Finally, in trace (v), after annealing the oxidized sample to 750 °C, the O 1*s* peak looks narrower and symmetrical again. The intensity as well as BE (530.2 eV) and FWHM are similar to those in (ii), i.e., after the deposition of a fresh layer of Cu. This agreement with the previously observed Zn and Cu features confirms the reduction of Cu_2O to metallic copper through this annealing procedure.

In Fig. 5, we show a series of spectra, with different emission angles, collected with the purpose of determining the oxide distribution within the thin layer. The spectra consider the Cu 2*p* states, after Cu deposition and oxidation (3 ML

TABLE III. BE of copper and oxygen features together with KE for the Cu LMM feature as measured by XPS, from different sources in the literature.

	BE (eV)					KE (eV) LMM Cu		
	Cu $2p_{3/2}$			O 1*s*				
Reference	Cu	CuO	Cu_2O	CuO	Cu_2O	Cu	CuO	Cu_2O
31	932.5	933.5		529.4			568.6[a]	
32	932.6		932.5		530.3			569.7[a]
33		933.8	933.3	530.3		918.5	917.1	916.3
34	932.7	933.6	932.5	529.6	530.4	918.6	917.8	916.5

[a]Binding energy.

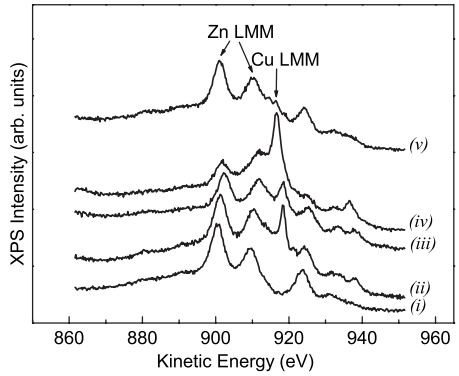

FIG. 4. Cu+Zn LMM spectra for (i) ZnO(0001)-Zn clean surface, (ii) after depositing 3 ML Cu at room temperature, (iii) the same sample after oxidation in oxygen plasma at 10^{-6} mbar, (iv) after an additional deposition of 3 ML Cu on the previously oxidized sample, and (v) the sample annealed to 750 °C.

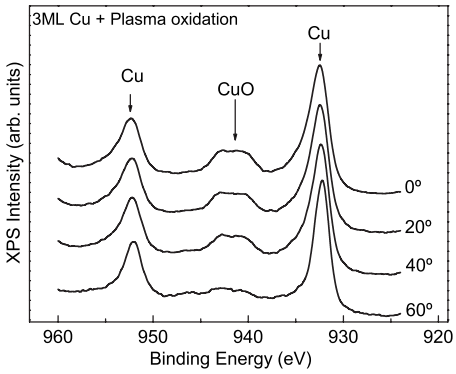

FIG. 5. Series of spectra of the Cu $2p$ states in the oxidized sample (3 ML Cu+plasma oxidation) as a function of emission angle. The XPS intensity of the satellite at 942 eV BE has its maximum at 0° and decreases gradually as the emission angle is increased. This result is consistent with Cu having a higher oxidation state closer to the interface.

Cu+plasma oxidation), as a function of the angle between the analyzer and the surface normal. The intensity variations in this type of measurements could be used to determine the composition distribution in a surface layer and has been used in the past for describing thin passive films on metals and for the detection of surface segregation in polymers.[32] In our data, the angular dependence of the XPS spectra manifests itself as a reduction of the relative intensity of the $2p_{3/2}$ satellite peak, together with a continuous narrowing of the Cu $2p$ peaks as the emission angle is increased. For larger emission angles, the resulting spectral data are more sensitive to the top layer composition.

The evident reduction of the relative intensity of the $2p_{3/2}$ satellite peak, together with a continuous narrowing of the Cu peaks as the emission angle is increased, indicates that the $2p$ transitions in the oxidized Cu clusters are composed of two distinguishable components: a high BE shoulder related to CuO and the main peak corresponding mostly to metallic Cu. The corresponding binding energies of the $2p_{3/2}$ components are 932.4 and 933.7 eV, respectively. The first of these components is related to metallic Cu and the second one to CuO. From this analysis, it is then possible to conclude that only a fraction of the copper in the clusters is found in a Cu^{2+} oxidation state and that part of it retains its metallic character.

The reduction of the intensity of the satellite peak for larger angles is then consistent with a gradient in the CuO concentration, with the higher oxidation states being closer to the ZnO interface. At the same time, the top parts of the clusters are more metallic, since the spectra for large angles are more consistent with metallic Cu. From this result, it is then clear that the stabilized ZnO surface does play an active role in the formation of the Cu oxide layer at this interface. These partially oxidized clusters show explicit evidence of a spatial segregation of these two components in the direction of the substrate normal. Similar gradient distributions have been reported by Schalow *et al.*[37] for a Pd/Fe_3O_4 catalyst. Their results are consistent with oxygen being reversibly accumulated in a thin Pd oxide layer, at the metal/oxide interface.

It is not unreasonable to think that there are traces of Cu_2O in the overlayer after the initial oxidation, since the free energy is minimized in the CuO-Cu reaction which forms Cu_2O. The great resemblance between the spectra of the clean $2p$ resonances of Cu and Cu_2O makes it very hard to discard this fact based solely on this information. Nevertheless, the main difference between them (Cu_2O and Cu) is seen in the LMM Auger spectra, as shown in Fig. 4. These spectra (traces ii and iii) are consistent with the top layer of the clusters being mostly metallic Cu.

The formation of Cu_2O is a temperature dependent process. All our experiments were carried out with the samples at room temperature, however, the different procedures used to form the oxides, plasma oxidation, and Cu redeposition are not equivalent. An oxygen-plasma source induces a milder temperature effect at the interface when compared with Cu evaporation from a crucible at 1100 °C. Our data indicate that this temperature difference at the interface could be enough to promote Cu_2O formation.[33]

Similar angular dependence measurements were also carried out for the case of Cu redeposition on the previously oxidized clusters [trace (iv) in Fig. 2]. The absence of an angular dependence of the $2p$ peaks is then consistent with a uniform distribution of Cu_2O throughout the film. Consistent with this measurement, there is almost no variation of the relative intensity of the corresponding satellite peaks. Thus, confirming that Cu_2O is uniformly distributed in the adsorbed film.

SUMMARY

We have studied the Cu/ZnO interface, crystalline structure, its oxidation, and the effects of annealing. The room temperature deposition of Cu on ZnO(0001) is known to induce the formation of islands or cluster of the adsorbed metal. Due to the potential applications of this particular system, it is then reasonable to verify the changes induced in these metallic particles by controlled temperature treatments under different atmospheres. We have concentrated our ef-

forts on the determination of the effects of oxygen on the electronic structure. The plasma oxidation of the Cu clusters, grown at different coverages, is consistent with the formation of CuO. Both the angular evolution of the CuO 2*p* satellites and the changes in shape and energy shifts of the primary peaks are indicative of the formation of an oxide with a higher concentration at the ZnO-cluster interface. The rest of the film, closer to the vacuum interface, is mostly metallic Cu [Fig. 6 (i)]. Upon further deposition of Cu onto the oxidized clusters, we can induce the formation of Cu_2O as a dominant component. The CuO features are almost undetectable after Cu redeposition. The new oxide is better recognized by its Auger LMM spectra.

By means of the procedure described, we can define the initial oxide stoichiometry and spatial distribution in the adsorbed clusters. Our first treatment (plasma oxidation) produces an interfacial oxide (CuO) and the second one (Cu redeposition) induces the formation of a uniform oxide in the clusters with Cu_2O stoichiometry [Fig. 6 (ii)].

Metallic oxides have been shown to have singular catalytic behavior, in particular, if the sizes involved are in the nanometer range, as is the case of a few monolayers of Cu in ZnO. If we can modify the catalytic properties by changing the stoichiometry of the oxides, we could enable other applications of these materials. It is also reasonable to assume that the actual chemical behavior of Cu/ZnO catalysts may be better described under realistic conditions, as oxide clusters such as the one we have shown to exist rather than pure metal, if the Cu clusters are exposed in the different processes to oxidation conditions.

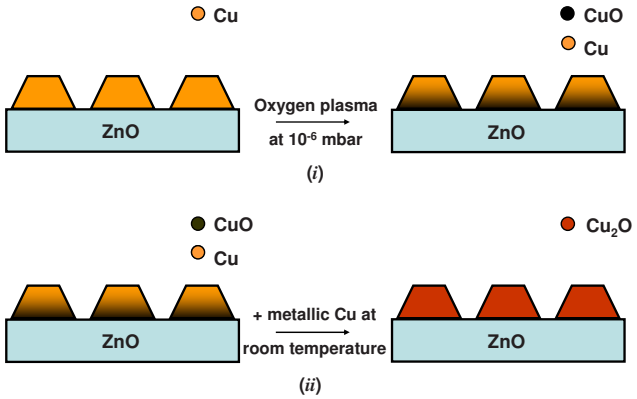

FIG. 6. (Color online) Schematic illustration of the different changes induced in the Cu/ZnO system by controlled temperature treatments under different atmospheres. The main compounds of the clusters are highlighted. The shape and apparent size of the clusters in the diagrams are arbitrary and not related to experimental results: (i) the Cu/ZnO system after an oxidation treatment in oxygen plasma at 10^{-6} mbar and (ii) the oxidized sample after an additional deposition of Cu.

ACKNOWLEDGMENTS

P.L. thanks the MECESUP program, Chile, for financing her graduate student stipend and a research visit to Tulane University, where these experiments were performed. Partial funding for this research was also provided by PBCT Grant No. ACT027, Chile.

[1] M. S. Spencer, Catal. Lett. **50**, 37 (1998).
[2] T. Fujitani and J. Nakamura, Appl. Catal., A **191**, 111 (2000).
[3] K. R. Harikumar and C. N. R. Rao, Appl. Surf. Sci. **125**, 245 (1998).
[4] G. Meitzner and E. Iglesia, Catal. Today **53**, 433 (1999).
[5] J. Agrell, M. Boutonnet, I. Melián-Cabrera, and J. L. G. Fierro, Appl. Catal., A **253**, 201 (2003).
[6] M. S. Spencer, Top. Catal. **8**, 259 (1999).
[7] Y. Choi, K. Futagami, T. Fujitani, and J. Nakamura, Appl. Catal., A **208**, 163 (2001).
[8] H. Purnama, T. Ressler, R. E. Jentoft, H. Soerijanto, R. Schlögl, and R. Schomäcker, Appl. Catal., A **259**, 83 (2004).
[9] Shin-Ichiro Fujita, Masahito Usui, and Nobutsune Takezawa, J. Catal. **134**, 220 (1992).
[10] Y. Toyoshima, M. Miyayama, H. Yanagida, and K. Koumoto, Jpn. J. Appl. Phys., Part 1 **22**, 1933 (1983).
[11] Y. Ushio, M. Miyayama, and H. Yanagida, Sens. Actuators B **B12**, 135 (1993).
[12] G. Eranna, B. C. Joshi, D. P. Runthala, and R. P. Gupta, Crit. Rev. Solid State Mater. Sci. **29**, 111 (2004).
[13] S.-J. Jung and H. Yanagida, Sens. Actuators B **37**, 55 (1996).
[14] Y. Nakamura, H. Zhuang, A. Kishimoto, O. Okada, and H. Yanagida, J. Electrochem. Soc. **145**, 632 (1998).
[15] Dang Hyok Yoon, Ji Haeng Yu, and Gyeong Man Choi, Sens. Actuators B **46**, 15 (1998).
[16] J. Yoshihara, J. M. Campbell, and C. T. Campbell, Surf. Sci. **406**, 235 (1998).
[17] J. Yoshihara, S. C. Parker, and C. T. Campbell, Surf. Sci. **439**, 153 (1999).
[18] L. V. Koplitz, O. Dulub, and U. Diebold, J. Phys. Chem. B **107**, 10583 (2003).
[19] F. Raimondi, J. Wambach, and A. Wokaun, Phys. Chem. Chem. Phys. **5**, 4015 (2003).
[20] B. Meyer and D. Marx, Phys. Rev. B **69**, 235420 (2004).
[21] S. T. Bromley, S. A. French, A. A. Sokol, C. R. A. Catlow, and P. Sherwood, J. Phys. Chem. B **107**, 7045 (2003).
[22] O. Dulub, U. Diebold, and G. Kresse, Phys. Rev. Lett. **90**, 016102 (2003).
[23] G. Kresse, O. Dulub, and U. Diebold, Phys. Rev. B **68**, 245409 (2003).
[24] Martin Kroll and Ulrich Köhler, Surf. Sci. **601**, 2182 (2007).
[25] O. Dulub, Matthias Batzill, and U. Diebold, Top. Catal. **36**, 65 (2005).
[26] J. F. Moulder, W. F. Stickle, P. E. Sobol, and K. D. Bomben, *Handbook of X-ray Photoelectron Spectroscopy* (Perkin-Elmer Corp., Eden Prairie, MN, 1992).
[27] Stephen V. Didziulis, Kristine D. Butcher, Susan L. Cohen, and Edward I. Solomon, J. Am. Chem. Soc. **111**, 7110 (1989).
[28] J. Ghijsen, L. H. Tjeng, J. van Elp, H. Eskes, J. Westerink, G. A. Sawatzky, and M. T. Czyzyk, Phys. Rev. B **38**, 11322 (1988).

[29] R. P. Vasquez, Surf. Sci. Spectra **5**, 262 (1998).
[30] S. Poulston, P. M. Parlett, P. Stone, and M. Bowker, Surf. Interface Anal. **24**, 811 (1996).
[31] G. Deroubaix and P. Marcus, Surf. Interface Anal. **18**, 39 (1992).
[32] John F. Watts and John Wolstenholme, *An Introduction to Surface Analysis by XPS and AES* (Wiley, West Sussex, England, 2003).
[33] S. Y. Lee, N. Mettlach, N. Nguyen, Y. M. Sun, and J. M. White, Appl. Surf. Sci. **206**, 102 (2003).
[34] P. D. Kirsch and J. G. Ekerdt, J. Appl. Phys. **90**, 4256 (2001).
[35] R. P. Vasquez, Surf. Sci. Spectra **5**, 257 (1998).
[36] V. E. Henrich and P. A. Cox, *The Surface Science of Metal Oxides* (Cambridge University Press, New York, 1994).
[37] T. Schalow, M. Laurin, B. Brandt, S. Schauermann, S. Guimond, H. Kuhlenbeck, D. Starr, S. Shaikhutdinov, J. Libuda, and H. Freund, Angew. Chem., Int. Ed. **44**, 2 (2005).